

SIMULATION OF DOMAIN SWITCH–TOUGHENING IN FERROELECTRIC CERAMICS

M. Kuna and A. Ricoeur

Freiberg University of Mining and Technology, Institute of Mechanics and Machine Components
09596 Freiberg, Germany

ABSTRACT

The influence of an electric field upon the fracture toughness of ferroelectric ceramics has been observed by many researchers. Our investigations deal with the calculation of ferroelectric/ferroelastic domain switching events near the tip of an electromechanically loaded crack. The calculations are based on a semi-analytical solution of the piezoelectric field problem yielding electric and mechanical fields around a crack tip. By means of a switching criterion, the specific work is related to a threshold value, deciding upon location and species of switching events. The thus determined extension of the fracture process zone is the basis for calculating changes in the fracture toughness due to domain processes. On this basis the influence of electric loads is investigated and results for two different orientations of material poling are presented. If the crack faces are aligned perpendicularly with the poling direction a positive electric field enhances the Mode-I fracture toughness. In the case of crack faces being orientated along the material poling axis the Mode-I fracture toughness is scarcely influenced by an external electric field, whereas the Mode-II toughness is strongly affected.

KEYWORDS

ferroelectrics, piezoelectrics, switch-toughening, smart ceramics

INTRODUCTION

Piezoelectric and ferroelectric ceramics find an application as actuators, sensors or ultrasonic transducers in many fields of technology. Because of their brittleness, problems of strength and reliability have to be major subjects of investigation. For the fracture analysis of smart ceramic structures a fracture criterion is needed, which relates relevant fracture quantities to the material toughness values, deciding on whether a given crack grows or not. In fracture mechanics of piezo- and ferroelectric solids, such a fracture criterion is not known yet. Within the scope of the K-concept, the loading of the crack tip can be described by the three classical stress intensity factors K_I , K_{II} and K_{III} and an additional electric intensity factor K_{IV} representing the singular behaviour of the electric displacement D_i in front of the crack tip [1]:

$$\begin{aligned}\sigma_{ij}(r, \theta) &= \frac{1}{\sqrt{2\pi r}} [K_I f_{ij}^I(\theta) + K_{II} f_{ij}^{II}(\theta) + K_{III} f_{ij}^{III}(\theta) + K_{IV} f_{ij}^{IV}(\theta)] \\ D_i(r, \theta) &= \frac{1}{\sqrt{2\pi r}} [K_I g_i^I(\theta) + K_{II} g_i^{II}(\theta) + K_{III} g_i^{III}(\theta) + K_{IV} g_i^{IV}(\theta)]\end{aligned}\tag{1}$$

A fracture criterion on the basis of the K-concept should be formulated by one single quantity K_A , being a function of the K-factors including K_{IV} . This quantity, representing the applied loading of

a fracture criterion equation, has to be compared to a material inherent critical value, the fracture resistance K_C . However, there is experimental evidence [2], that the critical value on the right hand side of the equation is a function of the electric field E_i and the poling direction P_i . It is assumed to be sufficient if only mechanical stress intensity factors are considered on the left hand side of the fracture criterion. The effect of an electric field is included in the material function on the right hand side and in the mechanical stress intensity factors by piezoelectric coupling. The fracture criterion is supposed to be

$$K_A(E_i) = K_C(E_i, P_i) \quad (2)$$

The micromechanical model, presented in this paper, has been developed as a tool to investigate the material function $K_C(E_i, P_i)$. Calculations also based on a micromechanical model recently have been published by Zhu and Yang [3,4]. In their work, piezoelectric field coupling is not considered, though.

CLOSED FORM SOLUTION FOR A CRACK IN AN INFINITE PIEZOELECTRIC

To find the eigensolutions of a piezoelectric material, the displacements u_i and electric potentials ϕ are represented by the function [5]

$$u_n = \begin{pmatrix} u_i \\ \phi \end{pmatrix} = \begin{pmatrix} A_i \\ A_4 \end{pmatrix} f(z) = A_n f(z) ; \quad z = x_1 + px_2 \quad (3)$$

which assumes the two field variables to depend on the coordinates x_1 and x_2 . Since derivations with respect to x_3 vanish, the strain tensor component ϵ_{33} and the component of the electric field vector $E_3 = \phi_{,3}$ are zero. The problem to be solved is governed by the following system of equations, which is derived from the field equations of linear elasticity and electrostatics as well as the constitutive equations of piezoelectricity:

$$\begin{aligned} C_{ijkl} u_{k,jl} + e_{ijl} \phi_{,jl} &= 0 \\ e_{ikl} u_{k,il} - \kappa_{il} \phi_{,il} &= 0 \end{aligned} \quad (4)$$

The elastic, piezoelectric and dielectric material constants are represented by the tensors C_{ijkl} , e_{ijl} and κ_{il} . In Eqn. 4 volumetric forces and charges are neglected. Inserting Eqn. 3 into Eqn. 4 yields a generalized eigenvalue problem revealing A_n and p as eigenvectors and eigenvalues, respectively. With the exception of x_3 being the material poling axis, which means that the $x_1 - x_2$ plane is the plane of isotropy, all four eigenvectors are linear independent. Thus, in Eqn. 3 the summation over all linear independent eigenvectors and $-$ values can be introduced to be inserted subsequently into the constitutive law of piezoelectricity. Furthermore, introducing a stress function χ_i ($\chi_{i,1} = \sigma_{i2}$, $\chi_{i,2} = -\sigma_{i1}$) and an electric displacement function θ ($\theta_{,1} = D_2$, $\theta_{,2} = -D_1$) and integrating with respect to z finally yields

$$\Phi_m = \begin{bmatrix} \chi_i \\ \theta \end{bmatrix} = M_{m\alpha} f_\alpha(z_\alpha) + \bar{M}_{m\alpha} \bar{f}_\alpha(\bar{z}_\alpha) \quad (5)$$

with the matrix

$$M_{m\alpha} = \begin{bmatrix} (C_{i2k1} + C_{i2k2} p_\alpha) A_{k\alpha} + (e_{1i2} + e_{2i2} p_\alpha) A_{4\alpha} \\ (e_{2k1} + e_{2k2} p_\alpha) A_{k\alpha} - (\kappa_{21} + \kappa_{22} p_\alpha) A_{4\alpha} \end{bmatrix} \quad (6)$$

Bars denote conjugate complex quantities. Eqn. 5 represents the general solution of the piezoelectric field problem. The solution of the crack problem is found adapting the function $f_\alpha(z_\alpha)$ to the boundary conditions of a Griffith crack with electrically impermeable and mechanically traction free crack faces. Furthermore, the crack faces, oriented parallel to the x_1 -axis of the crack coordinate system, are assumed to be free of electric charges. The external loads are accounted for by $T_m = [\sigma_{12}^\infty, \sigma_{22}^\infty, \sigma_{32}^\infty, D_2^\infty]$ comprising the stresses σ_{i2}^∞ and electric displacements D_2^∞ at infinity.

The function $f_\alpha(z_\alpha)$ can be determined applying a Fourier transformation. Finally, two sets of dual integral equations are obtained which are solved following Pohanka and Smith [6]. After resubstituting the stress and electric displacement functions χ_i and θ , the results for stresses and electric displacements

are [7]

$$\begin{aligned} \begin{bmatrix} \sigma_{k1} \\ D_1 \end{bmatrix} &= -\Re \left\{ M_{k\alpha} N_{\alpha m} p_\alpha \left[(z_\alpha^2 - 1)^{-\frac{1}{2}} z_\alpha - 1 \right] \right\} T_m \\ \begin{bmatrix} \sigma_{k2} \\ D_2 \end{bmatrix} &= \Re \left\{ M_{k\alpha} N_{\alpha m} \left[(z_\alpha^2 - 1)^{-\frac{1}{2}} z_\alpha - 1 \right] \right\} T_m \end{aligned} \quad (7)$$

$\Re\{..\}$ denotes the real part of a complex quantity, $N_{\alpha m}$ is the inverse of $M_{k\alpha}$. In Eqn. 7 the coordinates x_i (involved in the function z_α) are normalized with respect to the half crack length a .

CALCULATION OF FERROELECTRIC/FERROELASTIC SWITCHING ZONES

In the x_1 - x_2 plane it has to be distinguished between three different kinds of switching events. A tetragonal unit cell can switch 90 degrees clock- or anti-clockwise ($\pm 90^\circ$) or it can switch 180 degrees (180°). Switching events with a resulting orientation of the c -axis in the x_3 -direction i.e. parallel to the crack front are not under consideration. If ϕ is the angle between the c -axis of a unit cell and the crack faces, the change in polarization going along with a switching event can be described by the vector

$$\begin{aligned} \Delta \vec{P} &= b P^0 \begin{pmatrix} \sin(\phi + \varphi) \\ -\cos(\phi + \varphi) \end{pmatrix} \\ b &= \begin{cases} -\sqrt{2} & \text{for } +90^\circ \\ \sqrt{2} & \text{for } -90^\circ \\ -2 & \text{for } \pm 180^\circ \end{cases}, \quad \varphi = \begin{cases} +\pi/4 & \text{for } +90^\circ \\ -\pi/4 & \text{for } -90^\circ \\ +\pi/2 & \text{for } \pm 180^\circ \end{cases} \end{aligned} \quad (8)$$

with the amount of the spontaneous polarization of a unit cell P^0 . The specific electric work, which has to be supplied for the switching is calculated from

$$W_e = \int E_i dD_i \approx E_i \Delta P_i \quad (9)$$

The approximate solution of the integral is based on the assumption, that the electric field E_i remains unchanged in the course of the switching process. This implies, that the material constants are not influenced by the switching. Therefore the calculations have to be seen as a first order approximation. Furthermore in Eqn. 9 it is assumed, that the change in the electric displacement is dominated by the ferroelectric/-elastic switching, linear piezoelectric contributions are neglected.

Corresponding to the polarization switch vector of Eqn. 8, the change in strain due to the switching can be described by the tensor

$$\Delta \epsilon_{ij} = -\epsilon_D \begin{pmatrix} \cos 2\phi & \sin 2\phi \\ \sin 2\phi & -\cos 2\phi \end{pmatrix}; \quad \epsilon_D = \frac{c - a}{a_0} \quad (10)$$

The parameter ϵ_D contains the constants of the tetragonal and the cubic lattice a , c and a_0 . In the case of a 180° switching event ϵ_D is zero, since this species doesn't go along with a change in strain. The specific mechanical work, which has to be supplied for the switching is calculated from

$$W_m = \int \sigma_{ij} d\epsilon_{ij} \approx \sigma_{ij} \Delta \epsilon_{ij} \quad (11)$$

accounting for the same assumptions as in Eqn. 9. A simple switching criterion can be derived from Eqns. (9) and (11) relating the sum of specific mechanical and electric works to a threshold value, that approximately represents half of the area of a polarization hysteresis

$$\sigma_{ij} \Delta \epsilon_{ij} + E_i \Delta P_i \geq 2 E_C P^0 \quad (12)$$

The coercitive field is denoted by E_C . Eqn. 12 was first used by Hwang et al. [8]. It neglects contributions of grain boundary and domain wall energies [9]. The switching criterion has to be applied separately

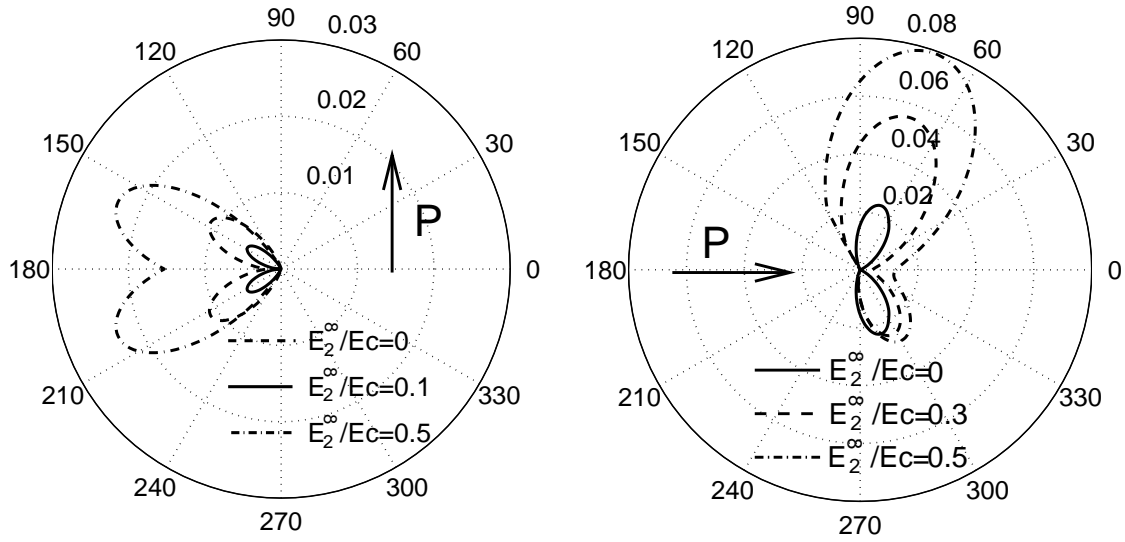


Fig. 1: Process zones for poling perpendicular (left) and parallel (right) to the crack faces

to the possible switching events, i.e. $\pm 90^\circ$ and 180° . For 180° events the first term in Eqn. 12 vanishes. Consequently, 180° switchings cannot be caused by mechanical fields. By means of the switching criterion it is decided, which one of the three events could occur at an arbitrary point in the $x_1 - x_2$ -plane. If there are several possibilities, the one variant will be chosen, which goes along with the highest amount of switching work. Stress tensor and electric field vector are inserted from the analytical solution for a crack, Eqn. 7, taking into account the constitutive law of piezoelectricity. Thus, a nonlinear algebraic equation for the determination of the switching zone boundaries is obtained. The union of the $+90^\circ$ and -90° zones is considered as the ferroelectric/–elastic fracture process zone, since it influences the fracture process by producing additional strain. There may be 180° switching events which dominate over possible $\pm 90^\circ$ events. Boundaries of the process zone being caused by an intersection of 180° and $\pm 90^\circ$ regions are calculated equating the switching energy densities of $\pm 90^\circ$ and 180° events:

$$\sigma_{ij} \Delta \epsilon_{ij}^{\pm 90} + E_i \Delta P_i^{\pm 90} = \sigma_{ij} \Delta \epsilon_{ij}^{180} + E_i \Delta P_i^{180} \quad (13)$$

Fig. 1 shows process zones for two different poling directions. The origin of the polar coordinate system coincides with the crack tip, the radius r is normalized with respect to the half crack length. The crack is coming from the left side with the crack faces lying at $\theta = 180^\circ$. In both diagrams three different electric loads are superimposed with a mechanical Mode-I loading. All calculations have been performed with the material constants of bariumtitanate. The electric loading is controlled by D_2^∞ , only. D_1^∞ , like e.g. σ_{11}^∞ results in a nonsingular, homogeneous electric displacement field and therefore is not relevant for fracture mechanics. E_2^∞ is approximately proportional to D_2^∞ and can be converted by the corresponding dielectric constant. Therefore, in Fig. 1 the electric loads are measured in multiples of the coercive field intensity ($E_C = 200$ V/mm). Fig. 1 shows, that the process zones for a poling perpendicular to the crack faces are smaller than for a parallel poling. Furthermore, it should be noticed that the process zones become asymmetrical if the directions of poling and electric loading are different as in the case of a parallel poling.

INFLUENCE OF SWITCHING EVENTS ON THE FRACTURE TOUGHNESS

The inelastic strain, caused by the $\pm 90^\circ$ switching events, can be interpreted as a residual strain thus leading to an additional loading or unloading of the crack. Its influence can be described by an additional stress intensity factor ΔK , which is defined as

$$\Delta K = \oint_S t_i h_i ds \quad (14)$$

The integration is performed over the boundary S of the process zone where the stresses t_i act due to a restraint of the residual strain. Eqn. 14 has been applied by McMeeking and Evans [10] to the investigation of transformation toughening. The function h_i describes the influence of a unit force in the crack tip near field on the stress intensity factors. Applying the method of complex stress functions for isotropic, elastic materials the effect of a force $F_i = [Q, P]^T$ is found [11]

$$K = K_I - i K_{II} = \frac{1}{\sqrt{2\pi}} \frac{1}{\kappa + 1} \left\{ (Q + iP) \left(\frac{1}{\sqrt{z_0}} - \kappa \frac{1}{\sqrt{\bar{z}_0}} \right) + \frac{(Q - iP)(\bar{z}_0 - z_0)}{2\bar{z}_0 \sqrt{\bar{z}_0}} \right\} \quad (15)$$

acting at the location $z_0 = x_{10} + i x_{20}$ (conjugate complex \bar{z}_0). For plane strain conditions it is $\kappa = 3 - 4\nu$ with Poisson's Ratio ν . Separating real and imaginary parts and taking into account the relations $K_I = F_i h_i^I$ and $K_{II} = F_i h_i^{II}$, we find in polar coordinates (r, θ) :

$$h_i^I = \frac{1}{2\sqrt{2\pi} r(1-\nu)} \begin{pmatrix} \cos\left(\frac{\theta}{2}\right) \left(2\nu - 1 + \sin\left(\frac{\theta}{2}\right) \sin\left(\frac{3\theta}{2}\right) \right) \\ \sin\left(\frac{\theta}{2}\right) \left(2 - 2\nu - \cos\left(\frac{\theta}{2}\right) \cos\left(\frac{3\theta}{2}\right) \right) \end{pmatrix} \quad (16)$$

Here, $r = |z_0|$ denotes the distance of the applied force from the crack tip. Bückner [12] interpreted Eqn. 16 as weight function, that's why h_i is often referred to as Bückner's weight function. For the Mode-II weight function it is found from Eqn. 15:

$$h_i^{II} = \frac{1}{2\sqrt{2\pi} r(1-\nu)} \begin{pmatrix} \sin\left(\frac{\theta}{2}\right) \left(2 - 2\nu + \cos\left(\frac{\theta}{2}\right) \cos\left(\frac{3\theta}{2}\right) \right) \\ \cos\left(\frac{\theta}{2}\right) \left(1 - 2\nu - \sin\left(\frac{\theta}{2}\right) \sin\left(\frac{3\theta}{2}\right) \right) \end{pmatrix} \quad (17)$$

In Eqn. (14) the stress vector can be replaced by the stress tensor using Cauchy's Theorem $t_i = \sigma_{ij} n_j$. Applying Hooke's Law, the stress tensor is expressed by the strain tensor, whereby the condition of isochoric deformations was taken into account ($\epsilon_{ll} = 0$):

$$\sigma_{ij} = \frac{E}{1+\nu} \left(\epsilon_{ij} + \frac{\nu}{1-2\nu} \epsilon_{ll} \delta_{ij} \right) = \frac{E}{1+\nu} \epsilon_{ij} \quad (18)$$

The strain tensor represents the additional strain, therefore being replaced by $\Delta\epsilon_{ij}$ from Eqn. (10). Eqn. (14) thus yields

$$\Delta K = \frac{E}{1+\nu} \oint_S \Delta\epsilon_{ij} h_i n_j ds = \frac{E}{1+\nu} \int_A \Delta\epsilon_{ij} h_{i,j} dA \quad (19)$$

The domain integral, which has been used for all calculations, is introduced using Gauß's Integral Theorem. E and ν are effective constants of an isotropic model material, which have to be calculated from the anisotropic elastic material tensor. Using polar coordinates, the integration with respect to r can be carried out analytically.

To take into account a statistical distribution of local unit cell orientations ϕ around the macroscopic poling angle ϕ_0 , a probability density function $w(\phi)$ is introduced. Inserting Eqns. 10 and 16 (17) into Eqn. 19 supplies an equation for the calculation of ΔK_I (ΔK_{II}). For ΔK_I it is for example

$$\Delta K_I = -\frac{3\epsilon_D E}{4\sqrt{2\pi}(1-\nu^2)} \int_{-\pi}^{\pi} \int_{-\pi}^{\pi} \sqrt{R(\theta)} \left[\cos\left(2\phi - \frac{7\theta}{2}\right) - \cos\left(2\phi - \frac{3\theta}{2}\right) \right] d\theta w(\phi) d\phi \quad (20)$$

$R(\theta)$ denotes the radius of the process zone boundary. If the crack grows by an amount Δa , the switching zone is also extended along the crack faces. If we assume, that no back switches occur in the course of the crack growth, there will be a homogeneous switching zone with the height of the original process zone ($\Delta a = 0$) enclosing the crack. In front of this background, R-curves can be calculated. Then the effective fracture toughness K_C^∞ is of interest:

$$K_{IC}^\infty = K_{IC}^{tip} - \Delta K_I ; \quad K_{IIC}^\infty = K_{IIC}^{tip} - \Delta K_{II} \quad (21)$$

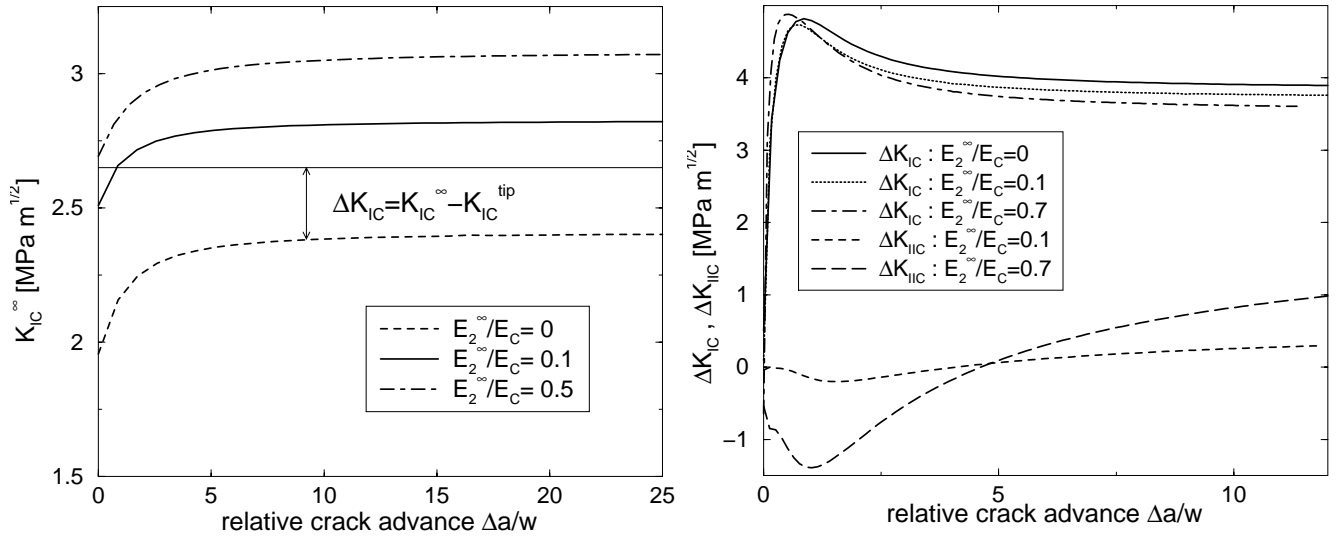


Fig. 2: Fracture toughness for poling perpendicular (left) and parallel (right) to the crack faces

It is the difference between a hypothetical (pure mechanical) fracture toughness at the crack tip K_{IC}^{tip} , K_{IIC}^{tip} neglecting switching effects, and the additional loading ($\Delta K > 0$) or unloading ($\Delta K < 0$) of the crack due to switching events, which is calculated from Eqn. 19.

Fig. 2 shows R-curves for the two poling directions depicted in Fig. 1. The crack length is normalized with respect to the largest extension w of the process zone perpendicular to the crack faces. Material constants and loading conditions are the same as in Fig. 1. In the left plot, the shape of the R-curves looks like expected. The calculations are based on a statistical distribution of the polarization angle with a maximum deviation from ϕ_0 of 30° and a Heaviside function as probability density function. K_I^{tip} was assumed as $2.65 \text{ MPa m}^{1/2}$. The screening effect $\Delta K_I = -\Delta K_{IC}$ obviously can be positive and negative. The Mode-I fracture toughness increases with increasing electric loading, ΔK_{II} is zero. The influence of electric fields shown in the diagram could be confirmed performing experiments on DCB specimens [2]. In the case of a parallel poling (right plot), little influence of the electric field can be observed for ΔK_{IC} , although the sizes of the process zones differ much. The reason lies in the fact, that around the crack tip within the section between 70° and 140° (Fig.1) the contribution of switching events to ΔK_{IC} changes its sign. So, a growing process zone produces both positive and negative contributions. The reason for the maximum in the R-curves is similar. When the crack starts growing it first passes the region of a positive contribution leading to a marked rise of ΔK_{IC} . During the crack growth negative contributions are produced leading to the maximum. In contrast with the case of perpendicular poling, there is a finite ΔK_{IIC} for parallel poling in connection with electric loads due to the asymmetry of the process zones. However, the amount of ΔK_{IIC} is smaller than the amount of ΔK_{IC} .

REFERENCES

1. Suo, Z., Kuo, C.M., Barnett, D.M. and Willis, J.R. (1992). *J. Mech. Phys. Solids* 40, 739.
2. Kuna, M. and Ricoeur, A. (2000). In: *Proc. of the SPIE Vol. 3992*, p. 185, Lynch, C.S. (Ed.).
3. Yang, W. and Zhu, T. (1998). *J. Mech. Phys. Solids* 46(2), 291.
4. Zhu, T. and Yang, W. (1997). *Acta mater.* 45(11), 4695.
5. Park, S.B. and Sun, C.T. (1995). *Int. J. of Fracture* 70, 203.
6. Pohanka, R.C. and Smith, P.L. (1988). *Electronic Ceramics*. Marcel Dekker, New York.
7. Ricoeur, A. and Kuna, M. (2001). *J. Mech. Phys. Solids* – submitted.
8. Hwang, S.C., Lynch, C.S. and McMeeking, R.M. (1995). *Acta Metall. Mater.* 43, 2073.
9. Arlt, G. (1990). *Journal of Materials Science* 25, 2655.
10. McMeeking, R.M. and Evans, A.G. (1982). *J. Am. Ceram. Soc.* 65(5), 242.
11. Erdogan, F. (1962). In: *Proc. of the 4th U.S. Nat. Congress of Appl. Mech.*, p. 547.
12. Bückner, H.F. (1970). *Z. Angew. Math. Mech.* 50, 529.